1. Experimental Effort

1.1 Surface Deformation Parameters for Oscillatory Themocapillary Flows

Y. Kamotani

Case Western Researve University

SURFACE DEFORMATION PARAMETERS FOR OSCILLATORY THERMOCAPILLARY FLOWS

Y. Kamotani[1] and S. Yoda[2]

[1]Case Western Reserve University, Cleveland, OH 44106, USA
[2]National Space Development Agency of Japan, Tsukuba, Ibaraki, Japan

ABSTRACT

Free surface deformation parameters are proposed herein to specify the onset of oscillations for various thermocapillary flows. The parameters are based on the assumption that free surface deformation plays an important role in the oscillation mechanism. It is shown that available experimental data for the onset of oscillations, including those taken in microgravity, can be correlated by those parameters well.

1. INTRODUCTION

Thermocapillary (or Marangoni) flow is known to become oscillatory (time-periodic) under certain conditions. Many experimental data are available concerning the onset conditions of oscillations, mostly for liquid bridges of high Prandtl number fluids. Numerical and stability analyses have also been performed by various investigators. Despite those investigations, the cause of oscillations is not yet fully understood. The dimensionless parameter directly related to thermocapillary driving force is Marangoni number (which will be defined later) and many investigators use critical Marangoni numbers to define the onset of oscillations. However, some ground-based data and microgravity data, covering wide conditions, do not support the existence of critical Marangoni numbers. This finding is only for high Prandtl number fluids at present because not enough experimental information is available for low Prandtl number fluids.

The objective of the present paper is to propose oscillation mechanisms involving free surface deformation for high Prandtl number fluids, and dimensionless parameters based on the physical models are derived to specify the onset of oscillations. Three different configurations are considered herein (see Fig. 1): liquid bridge, cylindrical container with a cylindrical heater along the centerline,

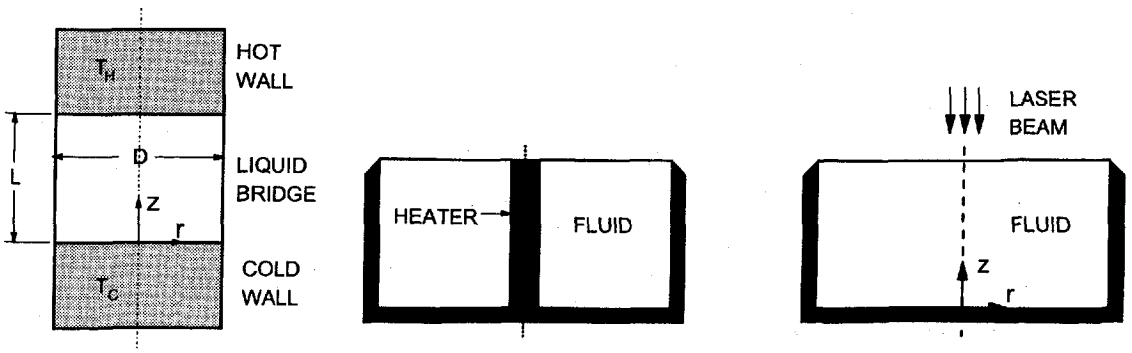

(a) HZ configuration (b) CT configuration (c) CF configuration

Fig. 1 Three experimental configurations

and cylindrical container with external laser heating. In all cases, the flows are known to become oscillatory, and the conditions for the onset of oscillations have been investigated in normal gravity as well as in microgravity. We have already analyzed all those cases separately (Kamotani et al., 1998, 1999a, 1999b). The results from those studies are compared herein to show that the concept of surface deformation parameter is universally valid.

2. BASIC STEADY FLOW FIELDS

Some important features of steady thermocapillary flows in the aforementioned three configurations are discussed first based mainly on numerical analysis. In the following, the liquid bridge (or half-zone) configuration, the cylindrical configuration with submerged heater, and the cylindrical configuration with laser heating are designated as HZ, CT and CF configurations, respectively, for short. We assume that buoyancy and gravity are negligible and that heat loss from the free surface is not significant. Then, the following dimensionless parameters are important for steady thermocapillary flow if the free surface is assumed to be flat and undeformable: Marangoni number $Ma= \sigma_T \Delta TL/\mu\alpha$, Prandtl number $Pr=\nu/\alpha$, and aspect ratio Ar=L/D in the HZ case and Ar=D/L in the CT and CF cases, where ΔT is the imposed temperature difference (T_h - T_c), μ is the fluid dynamic viscosity, ν is the kinematic viscosity, and α is the fluid thermal diffusivity. L is the column length for the HZ case and the container radius for the CT and CF cases. D is the column diameter for the HZ case and the container depth for the CT and CF cases. The heater radius in the CT case and the heating zone radius in the CF case are represented by Hr (heater ratio)=R_h/L.

The computed surface velocity and temperature distributions are shown for various values of Ma in Figs. 2-4. The velocity is non-dimensionalized by $\sigma_T \Delta T/\mu$, and the temperature is made dimensionless as $(T-T_c)/\Delta T$.

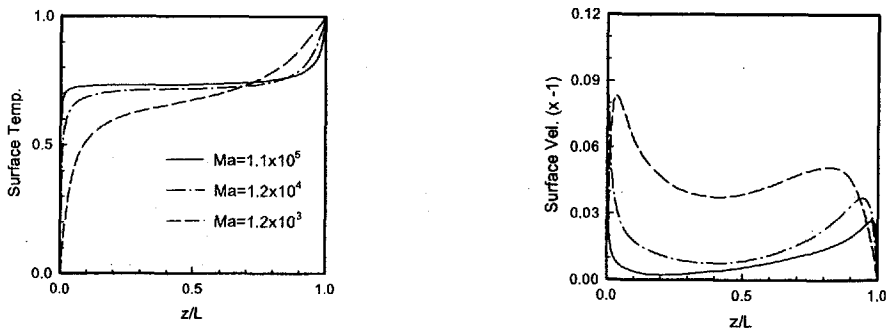

Fig. 2 Surface temperature and velocity distributions for HZ configuration (Ar=0.7, Pr=50)

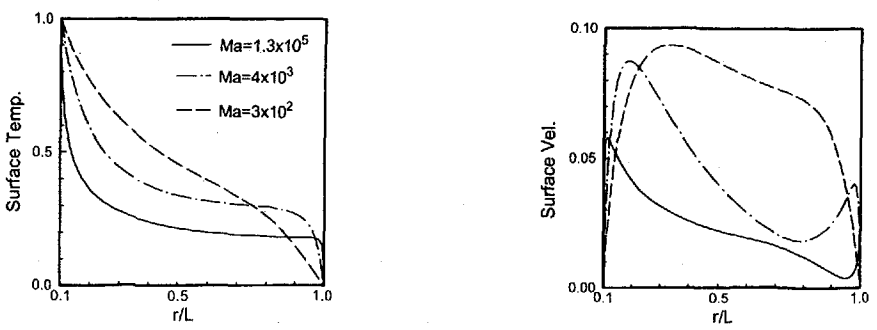

Fig. 3 Surface temperature and velocity distributions for CT configuration (Ar=1.0, Pr=20, Hr=0.1)

In the case of HZ (Fig. 2) and CT (Fig. 3) configurations, when Ma becomes large, convection causes large surface temperature changes near the hot and cold walls, called hot and cold corners herein, with a relatively uniform temperature region in between. As a result, relatively large thermocapillary driving forces exist in those corner regions and the surface velocity has a peak in each of those regions. The thermocapillary force in the cold corner is not effective in driving the whole flow because it is directed towards the cold wall, so we are mainly interested in the hot corner. As Figs. 2 and 3 show, the extent of hot corner shrinks and the peak (dimensionless) velocity decreases with increasing Ma. In the CF configuration (Fig. 4), the radial location where the surface velocity becomes maximum is fixed by the heating zone size, but the maximum velocity decreases with increasing Ma as in other cases.

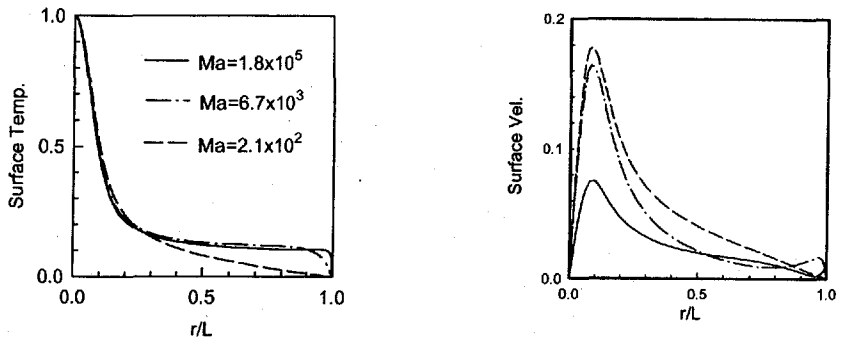

Fig. 4 Surface temperature and velocity distributions for CF configuration (Ar=1, Pr=20, Hr=0.1)

In the HZ and CT cases the hot corner shrinks with increasing Ma because the thermal boundary layer along the hot wall becomes thinner (Kamotani et al., 1998, 1999b). In the CF case the surface velocity decreases with increasing Ma because the velocity boundary layer along the free surface in the heated region becomes thinner (Kamotani et al., 1999a). Therefore, the common feature for all three cases is that the region where a large surface temperature gradient exists shrinks and the dimensionless velocity decreases with increasing Ma. This feature exists only for high Pr fluids. Because of this feature, the flow stays viscous-dominated even at high Ma (or Reynolds number R_σ=Ma/Pr).

In the HZ case, the whole flow is mainly viscous-dominated in the range of Ma where the flow is known to become oscillatory. The important quantities for the oscillation mechanism to be discussed later are the maximum velocity (U_0) and its axial location from the hot wall (Δ). Based on scaling and numerical analyses (Kamotani et al., 1998) they can be expressed, for a given Ar, as:

$$\mu U_0 / \sigma_T \Delta T \sim Ma^{-1/7}, \quad \Delta / L \sim Ma^{-1/2} \qquad (1)$$

In the CF configuration, the heating is very concentrated so that the flow is strong in the vicinity of the heated zone but much weaker in the rest of the flow field. In the range of R_σ where the flow is known to become oscillatory, there exist both velocity and thermal boundary layers along the free surface in the heated region. The bulk flow outside the heated region is mainly driven by the relatively small driving force outside the heated region and, as a result, the bulk flow is slow and viscous-dominated. In the CF configuration, the important quantities for the oscillation mechanism are the peak surface velocity (U_0) and the thermal boundary layer thickness (δ_{TH}) in the heated region, and the bulk flow velocity (U_b). They scale, for a given Ar, as (Kamotani et al., 1999a):

$$\mu U_0 / \sigma_T \Delta T \sim (\sigma_T \Delta T R_h / \mu\nu)^{-1/3}, \quad \delta_{TH} / R_h \sim (\alpha / R_h U_0)^{1/2}$$

$$U_b L / \alpha \sim (\sigma_T Q / k\mu\alpha)^{2/3} \qquad (2)$$

where Q is the total heat input and k is the fluid thermal conductuvity.

The heated area, relative to the cooled area, in the CT configuration is small but not as small as in the CF configuration, however the hot corner shrinks with increasing Ma in the CT case. In the range of Ma where the flow is known to become oscillatory, the hot corner becomes so small that the whole flow is basicaly dominated by the bulk flow which is driven by the relatively small driving force outside the hot corner. The important quantities are the bulk velocity scale (U_b) and the thermal boundary layer thickness along the free surface (δ_{TS}). For a given Ar, Hr, and Pr, they are given as (Kamotani et al., 1999b):

$$\mu U_b / \sigma_T \Delta T \sim Ma^{-1/5}, \ \delta_{TS} / L \sim Ma^{-2/5} \qquad (3)$$

Those scaling laws, Eq. (1) - (3), are for steady flows, so they are valid up to the onset of oscillations.

3. OSCILLATORY FLOW FIELDS AND OSCILLATION MECHANISMS

With increasing ΔT the flow becomes oscillatory in all three cases. The oscillatory flow field is always three-dimensional. Although the details of oscillatory flow fields are different, one common feature for all three cases is the following. At any given radial plane (r-z plane in Fig. 1), the flow along the free surface is observed to become strong and weak alternately, called active and slow periods herein. In the active period, convection along the free surface towards the cold wall increases so that the surface temperature increases, and the opposite happens in the slow period. The active and slow periods occur at different times at different radial planes so that the oscillatory pattern appears to pulsate or rotate around.

It has been shown for all three cases that available experimental data taken over a wide range of container or liquid column dimensions, including those taken in microgrvaity, do not support the existence of critical Marangoni number. In all cases the Marangoni number at the onset of oscillations, for a given Pr, Ar, and Hr, increases with increasing dimension of the flow field. Since the variation of Ma at the onset of oscillations is shown to be large, at least several-fold, there seems to be a need for an important extra feature to explain this trend. It is important to note that most of the data are consistent, which suggests that the effects of particular experimental procedure of each test, such as the rate at which ΔT is increased, are not appreciable in those data.

Based on our past work, we believe that the extra feature is free surface deformation. Since the free surface deformation is very small during oscillations (detectable only after magnification), it is usually neglected. However, as discussed above, thermocapillary flows contain very small but important length scales when Ma is large, so that the deformation may not be negligible compared to those small length scales. The most important aspect of the present oscillation model is that the return flow does not respond to a change in the surface flow immediately because it takes a finite time to change the free surface shape and generate a sufficient pressure gradient for the return flow change. Based on this time-lag nature, the following physical models are proposed for the three cases considered herein. In order to explain the oscillation mechanism, the flow along the free surface is called surface flow and the bulk flow towards the heated region in the interior is called return flow. We focus on a fixed radial plane in the following discussion. As in the basic flows, the details of oscillation mechanism are different between the HZ, CT, and CF cases, so they are discussed separately.

We start with the STDCE tests because much experimental and theoretical information is available. In the CT and CF configurations, the region of interest is the hot corner where thin velocity and

thermal boundary layers exist along the free surface. Since the bulk flow is the main flow in both cases, an active period is initiated when a sufficient amount of extra hot fluid is transported from the hot corner to the bulk region to increase the driving force for the bulk flow. An important fact regarding free surface deformation is that the viscous normal stress plays an important role. At the free surface, the surface tension force balances the sum of pressure and normal stress. In Fig. 5 the computed free surface shapes are shown for steady flows, obtained with and without the normal stress. As the figure shows, in both CT and CF cases the pressure is negative near the hot corner (the surface flow is causing suction there), and thus the pressure acts to depress the free surface

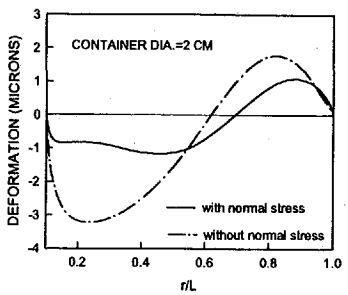

(a) CT configuration

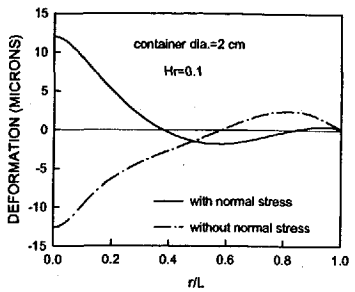

(b) CF configuration

Fig. 5 Free surface deformation for steady flow in CT and CF configurations

there. However, the normal stress counteracts the pressure appreciably so that it makes the free surface depression much smaller in the CT case and the free surface even bulges in the CF case (this has been observed experimentally). Since the pressure in the hot corner becomes more negative with increasing Ma, one would expect that the free surface depression increases with increasing Ma. However, since the normal stress increases with increasing Ma near the hot corner, the free surface becomes less depressed with increasing Ma in the CT case and becomes more bulged in the CF case, as shown in Fig. 6. This somewhat unusual behavior of the free surface near the hot corner is the key element in the oscillation mechanism. It is noted that the free surface depresses more in the hot corner with increasing Ma, when Ma is much smaller.

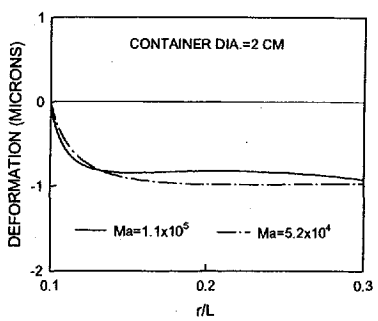

(a) CT configuration

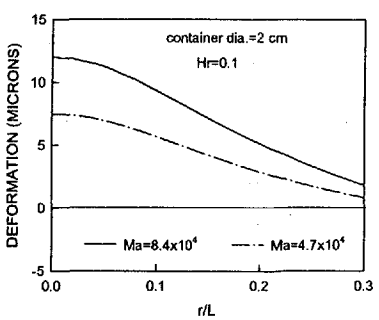

(b) CF configuration

Fig. 6 Free surface deformation for steady flow near hot corner

Suppose that the surface flow in the hot corner becomes stronger for some reason. Since the return flow does not respond immediately, the free surface deforms (depresses in this case). When the return flow responds, the free surface now is pushed back due to increased normal stress, which brings colder fluid from beneath the free surface. Then, the free surface temperature decreases, resulting in an increase in the temperature gradient along the free surface in the hot corner. The increased temperature gradient increases the surface flow further and the process continues with increasing surface flow. In the meantime, the decreased surface temperature in the hot corner in this

radial plane generates azimuthal surface temperature gradients, which induces thermocapillary flow toward this hot corner and brings more hot fluid from other hot corners. This is how an active period is initiated. The increased surface flow in the hot corner transports more hot fluid into the bulk region, and the bulk flow becomes stronger. In the active period, the surface temperature decreases in the hot corner but increases in the bulk region.

Eventually, the hot surface flow gets to the cold wall and excites the cold corner flow. The increased flow near the cold wall makes the return flow colder. As the stronger and colder return flow recirculates back to the hot corner, the surface temperature begins to decrease and the surface flow slows. This is the beginning of a slow period. In the slow period the surface temperature decreases in the bulk region but increases in the hot corner. Since the return flow is now colder than in the original state, the above process overshoots the original state. As the flow in the hot corner becomes weak, the thermal boundary layer thickness along the heater increases in the CT case, which expands the hot corner. Similarly, the velocity boundary layer thickness along the free surface increases in the CF case, which also expands the thickness of the hot corner. The increase of the hot corner extent eventually causes the surface flow to increase, and then the process described above initiates the next active period.

The situation is somewhat different in the HZ configuration. The free surface deformation for steady flow is shown in Fig. 7. In the HZ case, the peak surface velocity occurs at distance Δ from the hot wall, so the region around Δ is important. As Fig. 7 shows, the normal stress near that region again pushes back the free surface depression by the pressure force. Unlike the CT and CF cases, in which a thin thermal boundary layer exists along the free surface in the hot corner, there is no large temperature gradient normal to the free surface in region Δ. Therefore, the requirement to initiate the hot period is to increase the transport of hot fluid out of region Δ along the free surface. The flow is squeezed into very small corner region Δ with increasing Ma so that the (dimensionless) peak velocity decreases due to increased viscous effect. Therefore, if one could extend region Δ temporarily by some means, the velocity would increase and the flow along the free surface would become stronger.

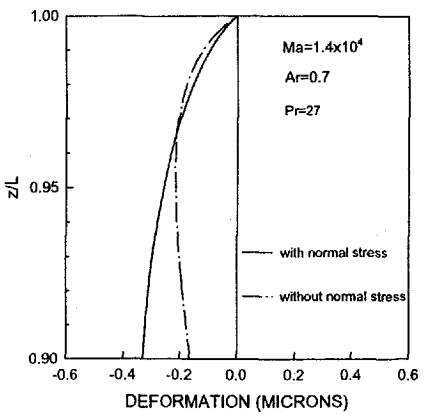

Fig. 7 Free surface deformation for steady flow in HZ configuration

Suppose again that the surface flow in region Δ becomes stronger for some reason. As before, the increased surface flow increases the transport of hot fluid out of region Δ, and also causes the free surface to depress slightly there. Since the surface velocity decreases outside this region (see Fig. 2), the fluid out of region Δ tends to accumulate just outside region Δ. Then, when the return flow responds to the above change and the normal stress pushes back the free surface, the flow near region Δ recirculates (a part of the hot fluid transported out of region Δ goes into the return flow towards

region Δ), which increases the surface temperature and extends region Δ. Thus, the recirculating cell increases its size and spreads toward the cold wall. This is the active period in the HZ configuration. The rest of the oscillation process is basically the same as in the above CT and CF cases.

In the above oscillation mechanisms for all three configurations, the free surface deformation is important only at the beginning of each active period.

4. SURFACE DEFORMATION PARAMETER (S-PARAMETER)

Based on the above physical models, we now derive parameters to determine the onset of oscillations. Since the details of the basic flow and oscillation mechanism are different among the three cases, the parameter for the onset of oscillations is different in each case.

In the CF configuration, the ratio of the free surface deformation to the thermal boundary layer thickness in the heated region must become finite to initiate the oscillation process. The amount of free surface deformation corresponding to a change in the surface flow is estimated by Kamotani et al. (1999a) as:

$$\delta_s \sim \left(\rho U_b^{\,2} R_h^{\,2} R/\sigma\right)^{1/2} \tag{4}$$

Then, from Eqs. (2) and (4), one obtains the following expression for the ratio of free surface deformation to thermal boundary layer thickness in the heated region for a given Ar :

$$S = \frac{\delta_s}{\delta_{TH}} \sim \left(\frac{\mu\alpha}{\sigma R}\right)^{1/2} \left(\frac{\sigma_T Q}{k\mu\alpha}\right)^{2/3} \left(\frac{\sigma_T \Delta T R_h}{\mu\nu}\right)^{1/3} \tag{5}$$

The above expression is called surface deformation parameter or S-parameter. From the above discussion, when the S-parameter is large enough, the oscillation process can be initiated. Figure 8 shows that our data taken under normal and microgravity conditions and for various values of Hr in the CF configuration can be well correlated by the above S-parameter.

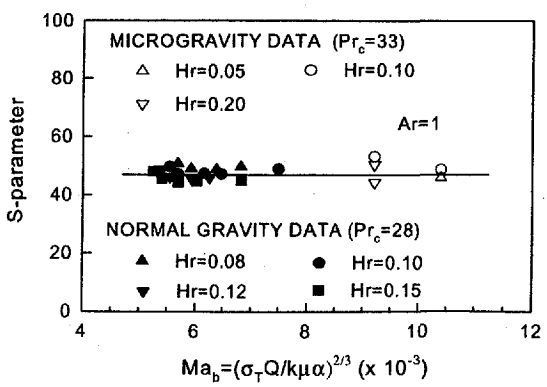

Fig. 8 Correlation of experimental onset conditions by S-parameter for CFconfiguration (Ma_b=bulk flow Marangoni number, Pr_c=Prandtl number evaluated at T_c)

Also, in the CT cofiguration, the ratio of the free surface deformation to the thermal boundary layer thickness along the free surface in the hot corner must become finite to initiate the oscillation process. The ratio is the S-parameter for the CT configuration. The surface deformation in the hot corner corresponding to a change in the surface flow is given as (Kamotani et al., 1999b)

$$\delta_s \sim \left(\frac{\rho U_b^2 R^3}{\sigma}\right)^{1/2} Ma^{-1/5} \qquad (6)$$

Then, from Eq. (3) and (6) one obtains the following expression for S-parameter for a given Ar, Pr, and Hr:

$$S = \frac{\delta_s}{\delta_{TS}} \sim \left(\frac{\rho\alpha^2}{\sigma R}\right)^{1/2} Ma \qquad (7)$$

In Fig. 9 our data taken in normal and microgravity are shown to be correlated well by the above parameter.

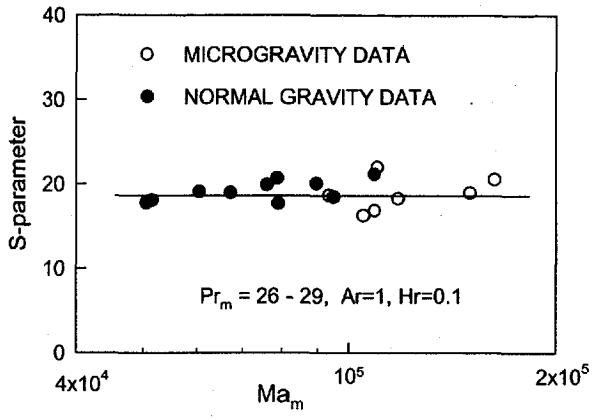

Fig. 9 Correlation of experimental onset conditions by S-parameter for CT configuration (subscript m for viscosity evaluated at mean temperature, $(T_h+T_c)/2$)

In the HZ configuration, we want to delay the return flow response in region Δ by surface deformation. The time to change the thermocapillary driving force in Δ scales with Δ/U_0, while the time delay caused by the surface deformation scales with δ_s/U_0, where δ_s is the amount of deformation. Actually, U_0 in δ_s/U_0 is the velocity difference between the surface and return flows caused by the time lag discussed above, so its magnitude is much smaller than U_0 but it still scales with U_0. Then, the time lag relative to the time of convection scales with δ_s/Δ. Actually, because of the above difference in U_0, the magnitude of time lag is much larger than the actual value of ratio δ_s/Δ. The amount of deformation corresponding to a change in the surface flow is obtained in Kamotani and Ostrach (1998) as

$$\delta_s \sim \left(\rho U_0^2 \Delta^3 / \sigma\right)^{1/2} \qquad (8)$$

Then, from Eqs. (1) and (8) one obtains the following expression for a given Ar:

$$S = \left(\frac{\delta_s}{\Delta}\right)^2 = \frac{\sigma_T \Delta T}{\sigma} \frac{1}{Pr} Ma^{3/14} \qquad (9)$$

In the HZ configuration, we call the square of ratio δ_s/Δ the S-parameter, to be consistent with our earlier work. Available data for the onset of oscillations in the HZ configuration are correlated in terms of S in Fig. 10. The figure shows that the S-parameter describes the onset conditions well.

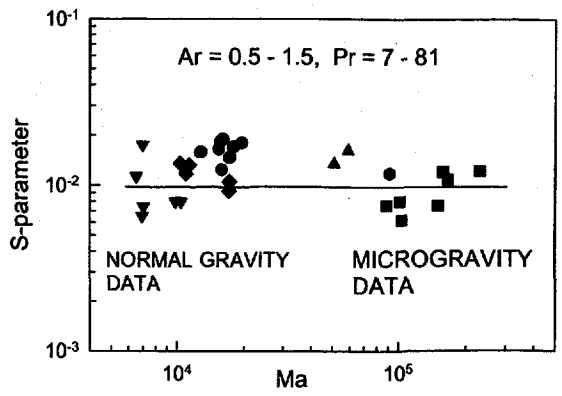

Fig. 10 Correlation of experimental onset conditions by S-parameter for HZ configuration

4. CONCLUDING REMARKS

As shown herein, the parameter, called S-parameter, based on the oscillation mechanism that includes free surface deformation can determine the onset of oscillations well in all three cases considered. Some details of oscillation mechanism are different among the three cases, but the basic feature is the same in that the free surface deformation, albeit small, changes the thermocapillary driving force significantly to initiate the oscillation process in which the surface flow becomes strong and weak alternately. At present, the oscillation mechanism has not been tested directly, so more work is being conducted on this subject.

5. ACKNOWLEDGMENTS

The first author (Y. K.) gratefully acknowledges the financial support from the National Space Development Agency of Japan (NASDA) for the present work.

6. REFERENCES

Kamotani, Y. and Ostrach, S., 1998, "Theoretical Analysis of Thermocapillary Flow in Cylindrical Columns of High Prandtl Number Fluids," Journal of Heat Transfer, Vol. 120, pp. 758-764.

Kamotani, Y. and Ostrach, S., and Masud, J., 1999a, "Oscillatory Thermocapillary Flows in Open Cylindrical Containers induced by CO_2 Laser Heating," International Journal of Heat and Mass Transfer, Vol. 42, pp. 555-564.

Kamotani, Y. and Ostrach, S., and Masud, J., 1999b, "Microgravity Experiments on Oscillatory Thermocapillary Flows in Cylindrical Containers," submitted to Journal of Fluid Mechanics.